Thermo-hydrodynamics of thin surface films in heterogeneous combustion

D. MEINKÖHN[1] and H. SPRENGEL[2]

[1]*HA Raumfahrtantriebe, Deutsche Forschungsanstalt für Luft- and Raumfahrt DLR, D-74239 Hardthausen, Germany; e-mail: dirk.meinkoehn@dlr.de*
[2]*Fakultät für Physik, Universität Bielefeld, D-33615 Bielefeld, Germany*

Abstract. Heterogenous reactions under transport control can be modelled in terms of a film of reaction products covering the reaction surface. Such a surface defines a unique direction in space which may be used to classify transport processes as transverse or longitudinal. Since crossed-gradient transport occurs, a Péclet number *Pe* is introduced, representing the ratio of the velocities characterizing transverse and longitudinal transport, with transverse transport being by film diffusion of some reacting species and longitudinal transport corresponding to film flow as with wetting processes. If the influence of viscosity is taken into account in terms of a Schmidt number *Sc*, the long-wave approximation for the evolution of thin films on reaction surfaces is shown to be equivalent to a distinguished limit $Pe \to 0$, $Sc \to \infty$, while keeping $1/(Sc\,Pe^2) = O(1)$. The long-wave approximation is derived by an application of the method of strained variables which leads to a film equation for the spatio-temporal evolution of the film thickness h which represents the crucial element for a complete solution of the thermo-hydrodynamics of the layer. Since film generation due to chemical reaction and film removal due to evaporation may compensate for certain thicknesses h, surface phases are found to occur which correspond to stationary layers of uniform thickness. The evolution of the surface layer is shown to be a generalized reaction-diffusion process, with surface waves representing dynamical transitions between surface phases.

Key words: thin films, surface phases, surface waves, heterogeneous combustion, surface ignition, surface extinction

1. Outline of the model

A combustion process is said to be heterogeneous if it is based on exothermal chemical reactions taking place on the surface of liquid or solid bodies. Such a reaction surface could be provided by condensed-phase fuel or oxidizer components, but also by the walls of the reaction vessel or some condensed-phase catalyst. Since the reaction sites in the case of heterogeneous combustion are confined to lie on a material surface, a major part in the overall reaction mechanism must be played by transport processes which are the object of the investigation to be presented. The surface normal of the reaction surface defines a reference direction in space. Therefore, transport processes may be classified as transverse or longitudinal, depending on whether they are parallel with the normal or in tangential directions.

A simple catalyzed transformation as displayed in Figure 1(a) may serve as an illustration.

This example, particularly, describes the overall transformation of species A into species B. It involves a number of consecutive steps which represent physical and chemical subprocesses. The reaction sites are supposed to lie on the surface of a solid body which is embedded in an ambient atmosphere containing the molecules of the 'fresh' reactant A and the product B. The reaction mechanism comprises transport of A in the ambient atmosphere towards the reaction surface, followed by adsorption $A \to A^{\#}$ and chemical transformation $A^{\#} \to B^{\#}$. Then there is surface transport $B^{\#} \to B^{\#}$, eventually followed by desorption $B^{\#} \to B$ and transport of B
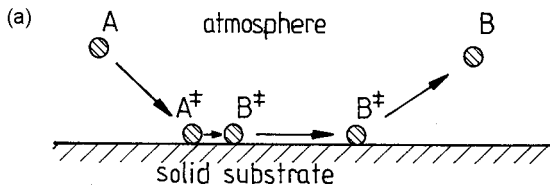
Figure 1(a). Heterogeneous Reaction $A \rightarrow B$ on a solid substrate, involving adsorption $A \rightarrow A^{\#}$, desorption $B^{\#} \rightarrow B$ and surface transport $B^{\#} \rightarrow B^{\#}$.
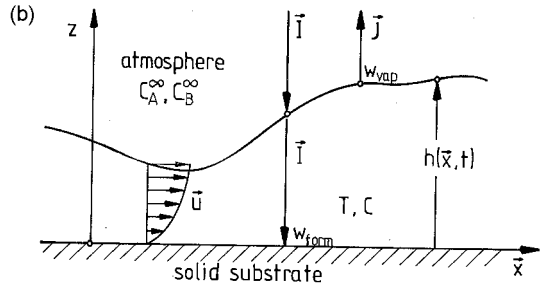
Figure 1(b). Continuous liquid film of reaction products screening the reaction surface on the solid substrate ($\vec{I}$ flux of fresh reactants, $\vec{J}$ flux of evaporated products, $\vec{u}$ velocity field, h film thickness, w_{form} rate of film formation, w_{vap} rate of film evaporation).

away from the reaction surface in the ambient atmosphere (for a more elaborate discussion of further examples, compare [1]). The adsorbed product molecules $B^{\#}$ effectively screen the reaction surface by blocking to a certain extent the access of the incoming A-molecules to the reaction sites, with the extent of the screening depending on the surface coverage c_s of B-molecules. In our model, this screening effect is assumed to be caused by a continuous surface layer of thickness h, formed by the reaction products. Consequently, the surface cover of product molecules is taken to represent a thermodynamic phase, to be described in terms of continuum-theoretic concepts. To reach the reaction sites covered by the layer, the fresh reactant A has to cross the layer by convection-diffusion processes, with the screening effect due to the transport resistance of the layer.

If $\bar{V}$ designates the molecular volume of the product species B, the layer thickness h is given by:

$$h = \bar{V} c_s. \tag{1}$$

For a sparse molecular coverage of the surface, h will be less than a molecular diameter. Surface layers with thicknesses which are measured on some microscopic scale defined in terms of the molecular diameter are termed 'microscopic'. In our model, microscopic layers are therefore taken as 2-dimensional surface phases, since they are of macroscopic extension only in longitudinal directions along the surface. A continuous increase in the layer thickness from microscopic to macroscopic values corresponds to a continuous transition from 2-dimensional to 3-dimensional thermodynamics in the description of the layer. If h is restricted to be of microscopic thickness, then the transition from microscopic to macroscopic layers is expressed by

$$h \rightarrow \infty. \tag{2}$$

Equation (2) indicates that macroscopic thicknesses are reached from the range of microscopic thicknesses by way of an asymptotic limit. The transition range for which thicknesses change from microscopic to macroscopic values is termed 'mesoscopic'.

Microscopic layers with $h \rightarrow 0$ are modelled by taking them as a 2-dimensional ideal gas which represents a continuum as with the analogous 3-dimensional ideal gas. From a kinetic point of view, a continuous film is obtained from a molecular covering with the help of a

suitable averaging procedure. A thermodynamic description of even very sparse molecular coverings remains possible, since the individual molecules are 'collision'-coupled indirectly via the substrate on which they reside.

Due to the assumption of continuity for layers of all thicknesses, our model equations cover all thickness ranges alike, independent of whether they are microscopic or macroscopic. It is therefore possible to treat the evolution of nonuniform layers with strongly varying thickness, with strong nonuniformity giving rise to surface transport (also called 'lateral' transport [2]) like surface flow and surface diffusion. Such strong nonuniformity involving a transition in the layer thickness from microscopic to macroscopic values arises for instance in the form of drops (often called 'caps') and film ruptures. Our model equations are particularly designed to investigate the formation, spreading and retraction of surface drops and ruptures. It should be observed, though, that large surface patches which are macroscopic in extent and which are entirely devoid of a covering layer do not occur, due to the effect of the chemical reaction. Therefore, a 'dry spreading' [3] of the layer is not included.

Since our model treats both microscopic and macroscopic layers on the same continuum-theoretic footing, it allows to interpret the model equations for microscopic layers in terms of concepts defined for macroscopic layers. For instance, surface tension associated with the outer surface of a layer is defined for macroscopic thicknesses. In our approach, this surface-tension concept can be carried over to the case of microscopic layers.

Since reactant A is consumed due to chemical conversion, a transverse concentration gradient exists which drives the fresh molecules A towards the reaction sites on the catalyst surface. In order to reach it, A must traverse the surface layer. For this to occur, A must dissolve in the layer at its outer surface, followed by convective-diffusive transport across the layer to the reaction sites which are at the bottom of the layer. Chemical reaction then leads to an increase of the layer thickness due to the formation of $B^{\#}$-molecules. In our model, the adsorbed molecules $A^{\#}$ and $B^{\#}$ of Figure 1(a) are modelled in terms of a liquid layer, with $B^{\#}$ forming the liquid and $A^{\#}$ an admixture dissolved in it. The process of desorption $B^{\#} \to B$ of Figure 1(a) is modelled in terms of an evaporation process at the outer surface of the layer, leading to a reduction in layer thickness.

It is a primary proposition of our model that the screening effect of the surface layer is of controlling importance. This is to say that the model is based on the assumption of transport control which presumes that the characteristic transport times are much larger than the times characterizing reaction. This proposition allows the model to be formulated exclusively in terms of physical processes governing transport by diffusion and convection which are much better understood than the actual chemistry of heterogeneous reactions. In our model the screening effect turns out to be equivalent to a thickness-dependent reaction rate which is associated with a thickness-dependent rate of film formation $w_{\mathrm{form}} = w_{\mathrm{form}}(h)$.

In the same spirit, we assume that product transport in the ambient atmosphere is slow in comparison with the characteristic time of evaporation. Consequently, a liquid–vapour equilibrium is assumed to hold locally on the outer surface of the layer, so that the concentration of product molecules on the vapour side of the surface is given in terms of the saturated vapour pressure p_h^v which is a function of the thickness h for microscopic and mesoscopic layers.

If the concentration of product molecules is assumed to vanish at large distances from the layer, the rate of vaporization w_{vap} is therefore given by

$$w_{\mathrm{vap}} \sim p_h^v. \tag{3}$$

Our approach in terms of a continuous surface layer of nonuniform thickness h and the fluxes I, J of species A, B is illustrated in Figure 1(b).

The processes of film formation (caused by chemical reaction) and film removal (caused by desorption or evaporation) are determined by transport processes in a direction which is transverse, due to their driving gradients. Lateral transport, like surface diffusion [2] or convective film flow [4], is longitudinal. If transverse transport is characterized in terms of a velocity v_0, longitudinal transport in terms of a velocity v_s, the ratio $Pe = v_0/v_s$ may be formed which represents a Péclet number. Our model is intended to treat heterogeneous combustion in terms of a superposition of transverse and longitudinal layer transport for which $Pe \ll 1$, indicating that transverse transport is supposed to be very slow in comparison with longitudinal transport. The assumption of $Pe \ll 1$ also arises in the similar case of convective diffusion in liquid boundary layers [5, 6]. For our model, v_s will be shown to have the properties of a sound velocity which characterizes the propagation of thickness perturbations in longitudinal directions. The particular aim of this paper is to investigate the range of mesoscopic layers which are of significance due to their intermediate position between the two qualitatively different ranges of microscopic and macroscopic layer thicknesses. For mesoscopic layers, v_s is given by a closed expression derived with the help of the Deryagin's disjoining pressure [3].

If the reaction surface is covered with a nonuniform layer, it is 'non-equiaccessible' [5, 6] for the reactants in the ambient atmosphere. For thin continuous layers, concepts may be used which were developed for convective diffusion in liquid boundary layers [5, 6] and for flow phenomena in shallow water [7]. These concepts allow to model the thermo-hydrodynamics of thin films in terms of linear field equations for state variables which are strongly coupled due to nonlinear boundary conditions. Particularly, we generalize the long-wave approximation for thin films by Burelbach, Bankoff and Davis [4], in order to include growth and decay of surface layers due to chemical reaction, desorption and evaporation.

For nonuniform surface layers, lateral transport leads to typical combustion phenomena like ignition and extinction which characterize the propagation of combustion. Since it is accompanied by a change in surface-layer thickness, lateral transport represents a surface wave. If such a surface wave, for instance, brings about a spreading reduction in layer thickness, an increase in reaction will spread on the surface because of the diminished screening capacity of the layer. For heterogeneous combustion, such a surface wave is therefore associated with with 'surface ignition' (or 'surface inflammation' [6]). The converse phenomenon, *i.e.* a surface wave bringing about a spreading increase in layer thickness, corresponds to surface extinction.

2. A motivating example

A typical application of our model is in the field of fuel-particle combustion where oxides are often found to form a nonuniform layer covering the fuel surface which corresponds to the site of the reaction [1]. Examples are provided by the cases of boron combustion [8] and aluminium combustion [9].

For boron (melting point 2450 K, boiling point 3930 K), surface combustion is observed. Since the boiling point of boric oxide B_2O_3 (melting point 723 K, boiling point 2316 K) is lower than the melting point of solid boron, combustion of boron involves two consecutive stages

- an ignition stage at temperatures below 2316 K, for which the solid boron is covered with a liquid layer of boric oxide which is macroscopic in thickness;

- a stage of full-fledged combustion at temperatures beyond 2316 K, but below the boron boiling point due to the high value of the heat of vaporization for boron, with surface burning rather than the usual vapour-phase burning.

In both stages, the reaction products are formed at the boron surface. Both stages therefore involve an oxide film covering the reaction surface which the oxygen of the ambient atmosphere must traverse. Whereas in the first stage the film may be of macroscopic thickness, for the second stage only microscopic thicknesses occur which characterize an adsorption layer.

For ignition to be successful, a transition from the first to the second stage needs to be achieved, while extinction corresponds to the converse phenomenon.

If the adsorption layer is taken to represent a 2-dimensional continuum, a reaction model may be set up as outlined in Section 1. Particularly, the conversion of boron to boron oxide involves the atmospheric oxygen to be dissolved in the liquid oxide layer and to be transported across the layer to the reaction sites on the boron surface which is underneath. There are many examples of transport-dominated growth of oxide films, even at elevated temperatures [10], but, in the temperature range for boron combustion, experiments are difficult to perform, particularly on account of the presence of oxygen. In the case of boron combustion there is thus still some dissent as to the exact values of the relevant transport parameters, specifically as to the solubility and the diffusivity of oxygen in liquid boric oxide [8, 11]. Oxygen diffusivity is found to be roughly $(2 \div 4) \cdot 10^{-6} \, \text{m}^2/\text{s}$ at 2000 K, whereas solubility follows if a particular solution theory model is assumed. Worked examples are ideal dilute-solution theory leading to Henry's law [12] or regular solution theory for higher oxygen partial pressure [13].

The relevant transport parameters for liquid boron oxide η, k, D (viscosity, thermal diffusivity, diffusivity for O_2 diffusion) are temperature-dependent, as shown by experimental investigations (for η see [16], for k see [14], for D see [8]). Since calculations [15] demonstrate that the temperature difference T_{ch} across the film is small in comparison with film and substrate temperatures ([15] shows $T_{ch} < 17$ K for substrate temperatures in the range of 2000 K), constant values η_0, k_0, D_0 will be assumed.

A measure of the relative importance of longitudinal as well as transverse viscous flow of oxide (containing the dissolved oxygen) in comparison with oxygen diffusion is provided by the Schmidt number Sc. For boron oxide at about 2000 K, the kinematic viscosity ν_0 is equal to $2 \cdot 72 \, \text{m}^2/\text{s}$ [16], and the diffusivity D_0 of oxygen is chosen to be $4 \cdot 10^{-6} \, \text{m}^2/\text{s}$ [17], whereby $Sc = \nu_0/D_0$ results in the range of 10^6. The fact that $Sc \gg 1$ will be used in the long-wave approximation as introduced in Section 4.

The models for boron and aluminium particle combustion [8, 9] are both marred by an important shortcoming in that they do not provide for symmetry-breaking. This implies that for spherical particles in a stagnant atmosphere the symmetry is to remain spherical for all stages of the combustion process. But there is ample experimental evidence to the contrary, *i.e.* for symmetry breaking, as evidenced by the strongly curved tracks of igniting and combusting boron and aluminium particles (see *e.g.* [18, 19]). In the case of aluminium, surface nonuniformity leading to macroscopic oxide caps is observed [20] which has been identified as the primary source of excessive slag formation in rocket boosters with fuel grains heavily laden with aluminium.

Layer nonuniformity leads to surface transport, since surface gradients of thickness, temperature and oxygen concentration arise. For layers which are thin enough, gradients in the internal pressure are essentially due to nonuniformities in the layer thickness, leading to surface convection or surface diffusion as the case may be. The functional dependence of the

internal pressure on the layer thickness remains yet to be determined in the case of oxide layers for boron and aluminium particles. It can be obtained from the corresponding adsorption isotherms, to be derived for various suitable temperatures. For an experimental investigation of the evolution of a liquid oxide film on solid boron, polarization ellipsometry could be tried, which has been successfully employed already in an investigation of boron-oxide films on platinum substrates [21].

For the internal pressure p_h in the transition region of mesoscopic thicknesses, its dependence on the layer thickness h is given in terms of an additive contribution, the so-called 'disjoining pressure' $\Pi(h)$ [22]. It has the general property of $\Pi \rightarrow 0$ for $h \rightarrow \infty$, with h measured on some microscopic scale (Equation (2)). Since there is as yet no general expression for Π in this range, a simple expression in terms of a Hamaker constant will be assumed (for a general idea of the possible values of the Hamaker constant, see [2]).

The dependence of p_h on the layer thickness will be used to define a sonic velocity $v_s = \sqrt{(h_0/\rho)\partial p_h/\partial h}$ which characterizes the longitudinal propagation of surface-waves. Since $Sc \gg 1$, transverse transport is characterized by the velocity $v_0 = D_0/h_0$ of diffusion. Therefore, a Péclet number $Pe = v_0/v_s$ can be introduced to compare transverse transport with surface-wave propagation. Section 4 will exploit the consequences of $Pe \ll 1$. For boron oxide, v_s is given once $p_h = p(h)$ is known. Generally, $\partial p_h/\partial h$ can attain large values for films which are thin enough [2].

The adsorption isotherms therefore govern longitudinal transport as well as adsorption and desorption (or, for thicker layers, condensation and evaporation). For macroscopic layers, King [15] uses a Clausius–Clapeyron expression for the vapour pressure p^v of boric oxide which is given in terms of the substrate temperature T_p as: $p^v = 1 \cdot 51 \cdot 10^8 \exp(-44000/T_p)$ [atm]. An indication of the influence of solid boron on the partial pressure of B_2O_3 is provided by the experimental results of Scheer [23].

Another driving force for surface flow is associated with the temperature and composition dependence of the surface tension for the liquid layer, resulting in thermal and solutal Marangoni effects. For liquid boron oxide, the thermal Marangoni effect has been experimentally determined for temperatures ranging from 770 to 2300 K [24]. Here, the surface tension is found to range from 70 to 120 dyn/cm. There are no experimental results as to the solutal Marangoni effect, but it is known to be generally much weaker than its thermal analogue.

3.   Thermo-hydrodynamics: field equations and boundary conditions

In order to set up a simple model, the heterogeneous combustion process is to take place on a solid support (the fuel, say, or a catalyst) with a plane surface defined to be the site of the reaction. This reaction surface is covered with a continuous liquid layer of nonuniform thickness consisting of reaction products, the layer separating the reaction surface from the gaseous reactants contained in an ambient atmosphere. The layer is taken to be bounded both at the bottom and at the top (the outer surface) by an interface that is assumed to be a Gibbs dividing surface [25]. With such an approach, a surface tension associated with the top surface of the layer is defined for all layers, *i.e.* even in the case of microscopic layer thicknesses. For a layer bounded by two dividing surfaces, the thermo-hydrodynamics are determined by boundary conditions which take the form of jump conditions [26]. The large difference in density, viscosity, species and heat diffusivity between the layer and the ambient bulk phases (the solid support and the ambient atmosphere) permits to formulate a 'one-sided model' for the layer alone [4].

Let z designate the transverse coordinate in the direction of the surface normal, x_1, x_2 being the longitudinal coordinates in tangential directions. Let $\vec{v}, T, C$ designate the film velocity, the temperature and the mass fraction of the reactant A which originates from the ambient atmosphere. Let w be the transverse component and u_1, u_2 the longitudinal components of $\vec{v}$. Then the following field equations model the thermo-hydrodynamics of an incompressible film of density ρ (Figure 1(b))

$$\nabla \cdot \vec{v} = 0, \tag{4}$$

$$(\partial_t + \vec{v} \cdot \nabla)C = \nabla^2 C, \tag{5}$$

$$(\partial_t + \vec{v} \cdot \nabla)T = (k_0/D_0)\nabla^2 T, \tag{6}$$

$$(\partial_t + \vec{v} \cdot \nabla)\vec{v} = (\nu_0/D_0)(-\nabla(p + \Pi) + \nabla^2 \vec{v}), \tag{7}$$

where k, D, ν designate the thermal diffusivity, the diffusivity of species A in the film liquid and the viscosity of the film. These parameters are functions of the temperature T, but for small temperature differences across the film they may be replaced by constant values k_0, D_0, ν_0 corresponding to an appropriate reference temperature T_0.

In Equation (7), p designates the difference between the thermodynamic pressure in a macroscopic film and the pressure p_∞ in the ambient atmosphere, whereas the contribution $\Pi(h)$ represents the so-called 'disjoining pressure' [3] which is a function of the thickness h and arises in microscopic and mesoscopic films due to van-der-Waals interaction between the molecules of the film and of the substrate. For mesoscopic films, the following expression has been derived for a simple case [22]

$$\Pi(h) = \alpha/h^3, \tag{8}$$

where α designates the so-called 'Hamaker constant'. For a transition from mesoscopic to macroscopic films $\Pi(h) \to 0$ according to (8), since $h \to \infty$ from (2). This expresses the physical fact that for bulk films, on account of their small range, van-der-Waals interactions between the molecules of the film and the molecules of the substrate give rise to a negligible contribution.

According to (4)–(7), the thermo-hydrodynamics of films are determined by the Lewis number $Le = \kappa/D$ and by the Schmidt number $Sc = \nu/D$. This results from a dimensionless representation of Equations (4)–(7), to be obtained if the following scaling assignments are made (primed variables are dimensional, unprimed variables are dimensionless)

$$\left. \begin{array}{llll} \vec{x}\,' = h_0\vec{x}, & z' = h_0 z, & t' = (h_0^2/D_0)t, & \vec{v}\,' = (D_0/h_0)\vec{v} \\ (p - p_\infty)' = (\rho\nu_0 D_0/h_0^2)p, & C' = C_{\mathrm{eq}}C, & (T - \theta_0)' = T_{ch}T. \end{array} \right\} \tag{9}$$

The following scales are used in the transformations of (9): h_0 = reference film thickness, ν_0, D_0 = reference values of viscosity and diffusivity, C_{eq} = equilibrium mass fraction of A in the liquid, determined *e.g.* by Henry's law, θ_0 = mean temperature of the solid substrate, T_{ch} = reference temperature difference for the surface layer. It should be noted that C' is dimensionless by definition since it represents a mass fraction. Thus, C is the scaled mass fraction associated with C' according to (9).

As with capillary waves, h_0 is meant to set a scale, so that long waves may be distinguished from capillary waves which differ as to the range of wave lengths λ. For long waves $\lambda \gg h_0$ is required. Restriction to long waves therefore implies restriction to large-scale structures.

According to the founding principles of our model, physicochemical equilibrium is assumed to hold locally at the top surface of the layer. By Henry's law, the mass fraction C_{eq} of the component A on the liquid side of the top interface is equal to the atmospheric mass fraction multiplied by a Henry constant. Since transport of A in the liquid layer is assumed to be controlling (*i.e.* is assumed to be very slow), the atmospheric concentration of A is taken to be a given constant.

On the gas side of the top interface, the local partial pressure of the layer material (the reaction product B) is taken to be equal to its saturation pressure p_h^v, in line with the assumption of transport of B in the ambient atmosphere controlling the evaporation process. Since far away from the top surface the atmospheric concentration c_B of B is assumed to vanish, a net evaporative mass flux J' is found to result. Similarly, due to the consumption of A at the bottom surface of the layer, a net mass flux I' of A is found to traverse the layer. A reference evaporative mass flux J_{ch} defined as

$$J_{ch} = k_0 \rho c_p \frac{T_{ch}}{h_0 L}, \tag{10}$$

is employed to make both mass fluxes dimensionless. In Equation (10), L designates the heat of vaporization and c_p the specific heat of the layer material. Consequently, the dimensionless mass fluxes I of A and J of B follow as

$$J' = J_{ch} J, \qquad I' = J_{ch} I. \tag{11}$$

For the flux J' in the ambient atmosphere we find

$$J' = \alpha_{ev}((c_B^s)' - c_B^\infty) = \alpha_{ev}(c_B^s)'. \tag{12}$$

In Equation (12), α_{ev} designates the transfer coefficient of B-molecules in the ambient atmosphere, with α_{ev} determined by the ratio of the atmospheric diffusivity of B and the effective distance beyond which the concentration is $c_B = c_B^\infty \simeq 0$. At the surface, the concentration c_B^s is given in terms of the saturation pressure p_h^v of B-vapour

$$(c_B^s)' = \frac{\mu_B}{R T_h'} (p_h^v)'. \tag{13}$$

Here μ_B designates the molar mass of species B, T_h' the layer temperature at the top surface, and R the universal gas constant.

The laws of Clausius–Clapeyron and of Kelvin may be combined to give p_h^v as

$$(p_h^v)' = \exp\left(-\frac{L}{R}\left(\frac{1}{T_h'} - \frac{1}{T_b}\right)\right) \exp\left(\frac{V_m}{R T_h'}\Pi'(h)\right). \tag{14}$$

According to Kelvin's law, an increase in internal pressure of the film leads to an increase in p_h^v, which for its part leads to an increase in the rate of evaporation according to Equations (12, 13). In (14), V_m designates the molar volume, whereas T_b corresponds to the boiling temperature of the liquid at a saturation pressure $p_h^v = 1$ bar above a bulk layer (*i.e.* $h = \infty$).

According to (9), the dimensionless form T_h of T_h' is obtained as

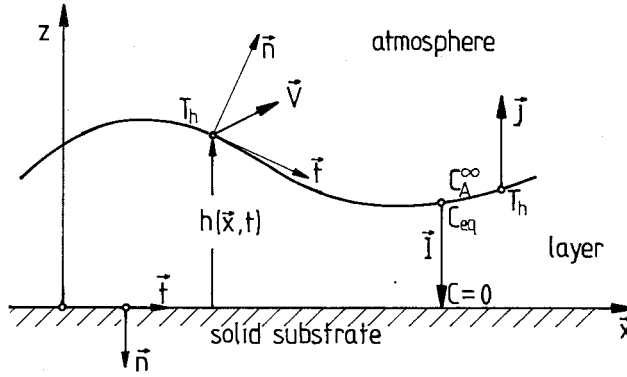$$T_h' = \theta_0 + T_{ch} T_h. \tag{15}$$

Figure 2. Definition of normal $\vec{n}$ and tangent $\vec{t}$ for the top and for the bottom surface of the layer ($\vec{V}$ velocity of the top surface, T_h temperature on the top surface).

Here, $\theta_0 =$ mean temperature of the solid substrate and $T_{ch} =$ a reference temperature difference in the layer.

For thin layers, the difference between between T'_h and θ_0 is small and can be expressed in terms of $\varepsilon = T_{ch}/\theta_0 \ll 1$ as follows

$$T'_h = \theta_0(1 + \varepsilon T_h). \tag{16}$$

The evaporation flux J' as given by (12) may then be linearized in terms of ε, which gives

$$J'(T_h, h) = J'(\theta_0, h) \left[1 + T_{ch} \frac{T_{ch} L}{R\theta_0^2} \left(1 - \frac{V_m \Pi'}{L} \right) \right]. \tag{17}$$

The dimensionless flux J therefore results as

$$J = \psi(1 + \Lambda T_h). \tag{18}$$

In (18), the following assignments are used

$$\psi = J'(\theta_0, h)/J_{ch} = \psi(h), \tag{19}$$

$$\Lambda = \frac{T_{ch} L}{R\theta_0^2} \left(1 - \frac{V_m \Pi'(h)}{L} \right) = \Lambda(h). \tag{20}$$

The fluxes as introduced with Equations (11) and (18) determine the kinematics of the top surface of the layer, which is given in terms of the surface normal $\vec{n}$ and the surface velocity $\vec{V}$ (Figure 2).

According to our model, the top surface represents a Gibbs dividing surface given by

$$z = h(x_1, x_2, t). \tag{21}$$

Its surface normal is $\vec{n} = \{-\nabla_s h, 1\}$ which is defined as pointing out of the film into the ambient atmosphere. Here, ∇_s designates the surface gradient (*i.e.* the surface nabla) that is given by

$$\nabla_s = \{\partial_{x_1}, \partial_{x_2}, 0\}. \tag{22}$$

The kinematics of the top surface are therefore determined by

$$\partial_t h - (\vec{n} \cdot \vec{V})\sqrt{1 + (\nabla_s h)^2} = 0. \tag{23}$$

In Equation (23), $V_n = (\vec{n} \cdot \vec{V})$ represents the normal velocity of the top surface of the layer.

At the top surface of the layer, the following boundary conditions (given in dimensionless form) must be imposed on the field equations (4–7)

$$\vec{n} \cdot (\vec{v} - \vec{V}) = E(J + I), \tag{24}$$

$$d\vec{n} \cdot [(\vec{v} - \vec{V})C - \nabla C] = I, \tag{25}$$

$$C = 1 \quad (i.e.:\ C' = C_{\text{eq}}). \tag{26}$$

In (24), $E = J_{ch}h_0/\rho D_0$ and in (25), $d = \rho D_0 C_{\text{eq}}/h_0 J_{ch}$. Both coefficients E and d are dimensionless.

The top surface of the layer corresponds to a liquid–vapour interface for which a stress boundary condition [26] may be formulated through use of the momentum fluxes $\vec{p}$ on the liquid side and $\vec{p}^v$ on the vapour side of the interface. The stressed state of the interface is expressed in terms of a surface tension σ. On the liquid side of the interface, $\vec{p}$ is determined by the flow field $\vec{v}$ whereas, analogously, on the vapour side $\vec{p}^v$ is determined by the vapour flow field $\vec{v}^v$.

The momentum flux $\vec{p}$ is given by

$$(\vec{p})' = -\mathbf{T}' \cdot \vec{n} + \rho \vec{v}'(\vec{v}' \cdot \vec{n}) \rightarrow \vec{p} = -\mathbf{T} \cdot \vec{n} + \frac{1}{Sc}\vec{v}(\vec{v} \cdot \vec{v}). \tag{27}$$

The momentum flux is scaled as: $(\vec{p})' = (\rho \nu_0 D_0/h_0^2)\vec{p}$. $\vec{n}$ designates the interface normal as defined in Figure 2, and $\mathbf{T}$ designates the stress tensor which is given as

$$\mathbf{T}' = -p'\mathbf{E} + \rho \nu_0 \mathbf{D}' \rightarrow \mathbf{T} = -p\mathbf{E} + \mathbf{D}. \tag{28}$$

Here, $\mathbf{E}$ designates the unit tensor, whereas $\mathbf{D}$ designates the deformation tensor given by the symmetric part $(\nabla \vec{v})^+$ of the tensor $(\nabla \vec{v})$

$$\mathbf{D} = (\nabla \vec{v})^+. \tag{29}$$

Equation (28) represents a constitutive equation for the film liquid, with p defined as representing the dynamic pressure as used in (7). Stress tensor $\mathbf{T}$ and deformation tensor $\mathbf{D}$ are scaled as follows (see Equation (9)): $\mathbf{T}' = (\rho \nu_0 D_0/h_0^2)\mathbf{T}$ and $\mathbf{D}' = (D_0/h_0^2)\mathbf{D}$.

The momentum flux $\vec{p}^v$ on the vapour side is obtained analogously by using $\vec{v}^v$, $\mathbf{D}^v$, $\mathbf{T}^v$, ρ^v, ν^v in (27–29).

If surface phases do not occur on the top surface of the layer, then momentum equilibrium in dimensionless form is expressed by

$$\vec{p} - \vec{p}^v + \sigma\kappa\vec{n} + \frac{d\sigma}{ds}\vec{t} = 0. \tag{30}$$

In Equation (30), the following scalings were used: $\sigma' = (\rho \nu_0 D_0/h_0)\sigma$, $\kappa' = \kappa/h_0$, $s' = h_0 s$. Here, $\vec{n}$, $\vec{t}$ designate the unit normal and the unit tangent vector as defined in Figure 2, s

designates the arc length of a path along the curved interface, whereas κ designates the mean curvature of the interface.

In terms of the mass transfer, $J' = \rho \vec{v}\,' \cdot \vec{n} = (\rho^v \vec{v}\,^v)' \cdot \vec{n}$ expresses continuity. For $\rho^v \ll \rho$, obviously

$$\vec{v}\,' \cdot \vec{n} \ll (\vec{v}\,^v)' \cdot \vec{n}.$$

Therefore, Equation (30) is found to give in dimensionless form

$$(\mathbf{T} - \mathbf{T}^v) \cdot \vec{n} + \frac{E}{Sc} J(\vec{v}\,^v - \vec{v}\,) + \sigma\kappa\vec{n} + \frac{\mathrm{d}\sigma}{\mathrm{d}s}\vec{t} = 0. \tag{31}$$

In (31), E as defined for Equation (24) was used, along with $Sc = \nu_0/D_0$.

Use of the no-slip boundary condition $(\vec{v}\,^v - \vec{v}\,) \cdot \vec{t} = 0$ and $\rho^v \ll \rho$ leads to

$$J(\vec{v}\,^v - \vec{v}\,) = J^2(1/\rho^v - 1/\rho)\vec{n} \simeq J^2\vec{n}/\rho^v.$$

For slow evaporation, the so-called 'vapour recoil' [4] may be neglected

$$J^2/\rho^v \simeq 0.$$

Therefore, the asymptotic limit

$$\rho^v/\rho \to 0, \qquad \nu^v/\nu \to 0$$

leads to the following stress boundary condition in terms of normal and tangential components

$$\vec{n} \cdot \mathbf{T} \cdot \vec{n} = -p + \vec{n} \cdot \mathbf{D} \cdot \vec{n} = -\sigma\kappa, \tag{32}$$

$$\vec{t} \cdot \mathbf{T} \cdot \vec{n} = \vec{t} \cdot \mathbf{D} \cdot \vec{n} = -\frac{\mathrm{d}\sigma}{\mathrm{d}s}. \tag{33}$$

Equations (32, 33) are given in dimensionless variables which are obtained by a scaling as defined by (9).

The nonscaled energy flux $\vec{s}$ is defined as

$$(\vec{s}\,)' = \vec{v}\,' \cdot \mathbf{T}' \cdot \vec{n} - \vec{v}\,' \cdot \vec{n}(\vec{v}\,')^2\rho/2 + k_0\rho c_p\nabla'T' \cdot \vec{n}. \tag{34}$$

In terms of $\vec{s}$ and $\vec{s}\,^v$, the energy boundary condition for the top surface of the layer is found to be

$$(\vec{s}\,)' - (\vec{s}\,^v)' + J'L = 0. \tag{35}$$

If $\vec{s}$ and $\vec{s}\,^v$ are expressed according to (34), then Equation (35) leads to

$$\vec{v}\,' \cdot \mathbf{T}' \cdot \vec{n} - (\vec{v}\,^v)' \cdot \mathbf{T}'^v \cdot \vec{n} - \tfrac{1}{2}J'((\vec{v}\,')^2 - ((\vec{v}\,^v)')^2) + k_0\rho c_p\nabla'T' \cdot \vec{n}$$
$$- (k_0\rho c_p)^v\nabla'(T')^v \cdot \vec{n} + J'L = 0. \tag{36}$$

Due to the no-slip boundary condition, the following may be assumed

$$\tfrac{1}{2}J[(\vec{v}\,')^2 - ((\vec{v}\,^v)')^2] \simeq -(1/2J)(J^2/\rho^v)^2 \to 0,$$

which corresponds to neglect of vapour recoil. Use of the conditions for the asymptotic limit

$$\rho^v/\rho \to 0, \qquad \nu^v/\nu \to 0, \qquad p^v/p \to 0$$

results in a neglect of the contributions of the stresses

$$J'L + k_0\rho c_p \nabla' T' \cdot \vec{n} - (k_0\rho c_p)^v \nabla'(T')^v \cdot \vec{n} = 0. \tag{37}$$

For slow evaporation, the heat transport on the vapour side may be modeled by Newton's law of cooling, expressed in terms of a Biot number *Bi* and a reference temperature T_∞ at large distance from the layer. For these settings, (37) is found to give

$$J'L + k_0\rho c_p \nabla' T' \cdot \vec{n} + Bi'(T' - T'_\infty) = 0. \tag{38}$$

Equation (38) states that the heat needed to vaporize layer material is provided by a heat flux out of the layer interior, while a certain loss of heat to the ambient atmosphere is also taken into account. The heat of dissolution of A-molecules in the layer liquid has been neglected because it is anticipated to give rise to a very small contribution.

In dimensionless form, (38) results as

$$J + \vec{n} \cdot \nabla T + Bi(T - T_\infty) = 0. \tag{39}$$

To obtain Equation (39), $Bi' = (LJ_{ch}/T_{ch})Bi$ and $T'_\infty = \theta_0 + T_{ch}T_\infty$ have been used. It should be noted that due to our definition of J_{ch} (see (10)), $k_0\rho c_p T_{ch}/h_0 L J_{ch} = 1$.

Equations (32, 33, 39) along with Equations (24–26) in conjunction with the field equations (see (4–7)) form the 'one-sided-model' of Burelbach/Bankoff/Davis [4]. It must be enlarged to account for the chemical reaction at the bottom surface of the layer due to which film material is generated.

At the bottom interface, the flux I of A-molecules which crossed the layer is converted into B-molecules, thereby adding to the liquid of the layer. At the bottom of the layer, therefore, the outgoing flux I is connected with an inflow J of layer material as

$$J = -\gamma I. \tag{40}$$

In (40), γ designates a conversion factor given by stoichiometry and molecular weights.

According to the primary assumption of our model, transport of A-molecules in the liquid layer is much slower than the chemical reaction converting A into B. Consequently, the concentration C of A vanishes at the bottom interface

$$C = 0. \tag{41}$$

The normal $\vec{n}$ at the bottom interface is also defined to point towards the exterior of the layer. It is therefore given as: $\vec{n} = \{0, 0, -1\}$ (Figure 2).

Consequently, at the bottom of the interface the fluxes I and J are given in dimensionless form as

$$\vec{n} \cdot \vec{v} = E(I + J) = -w, \tag{42}$$

$$d\vec{n} \cdot (\vec{v}C - \nabla C) = -d\vec{n} \cdot \nabla C = I = d\,\partial_z C. \tag{43}$$

The constants E, d appearing in (42) and (43) have already been introduced in (24) and (25) whereas w represents the z-component of the velocity $\vec{v}$ at the bottom interface.

For the range of macroscopic and mesoscopic thicknesses, the no-slip condition can be assumed at the bottom interface

$$\vec{v} \cdot \vec{t} = 0. \tag{44}$$

Consequently, in these thickness ranges, friction arises in two different ways: there is bottom friction due to (44), and there is viscous friction since $\nu_0 \neq 0$.

For microscopic continuous films, on the other hand, our model assumes that friction arises solely by way of viscosity, *i.e.* in the form of internal friction, while there is full slip of the film flow on the surface of the solid substrate. Consequently, the film viscosity ν_0 in the case of microscopic films is inversely proportional to the molecular mobility. A transition from mesoscopic to microscopic thicknesses therefore requires a corresponding gradual relaxation of the no-slip boundary condition, converting no-slip into full slip eventually for truly microscopic layers.

Finally, the thermal boundary condition at the bottom interface then gives ($z = 0$, $\vec{n} = \{0, 0, -1\}$)

$$\partial_z T - Bi_f(T - T_f) + Q_f \gamma I = 0. \tag{45}$$

In (45), heat loss into the solid substrate is modelled by Newton's law of cooling, expressed in terms of a Biot number $Bi_f' = (LJ_{ch}/T_{ch})Bi_f$. Here, $Q_f' = Q_f L$ designates a dimensionless heat of reaction (per mole of B produced), T_f designates a reference temperature deep in the interior of the solid substrate and $k_0 \rho c_p T_{ch}/h_0 L J_{ch} = 1$ due to Equation (10). If the boundary conditions at the top and at the bottom of the layer as given by Equations (18, 24–26, 32, 33, 39–45) are imposed on the solutions of the field equations (4–7), then the thermodynamic state of the film is obtained, as will be demonstrated in the next section with the help of the long-wave approximation. The evolution of the film is completely decoupled from the dynamics of the ambient atmosphere and the solid substrate.

4. The long-wave approximation

The field equations (4–7) for the interaction of film flow with film transport of species and heat form a difficult quasi-linear parabolic system of partial differential equations, for which the problem of well-posedness has not been generally resolved [7, 28]. The field equations are highly nonlinear and strongly coupled via the film thickness h and the boundary conditions, with h representing an unknown variable yet to be determined. The equations therefore correspond to a free-boundary problem.

In our treatment, the field equations and the boundary conditions are to be simplified through the use of methods adapted from shallow-water hydraulics [7, 28]. These methods prove to be particularly useful in providing a two-dimensional surface representation of the flow in films of any thickness, thus permitting a unified treatment of both three-dimensional bulk films and two-dimensional adsorption layers.

In its original formulation, shallow-water theory was designed for an investigation of flow dynamics in tubes and shallow open ducts, based on total neglect of all friction effects. Consequently, flows in shallow ducts are described by an Euler equation which expresses neglect of internal friction. If full slip of the liquid on the bottom of the duct is assumed, then

bottom friction is also neglected. Neglect of all friction is then found to lead to a hyperbolic film equation [7, 28] for the evolution of the film thickness h in time and space. This hyperbolic film equation is shown to possess weak solutions describing surface shock waves which take the form of hydraulic jumps, the so-called 'bores'.

For thin films, on the contrary, the effect of friction, and therefore of dissipation is of primary importance [3] and thus cannot be neglected. Consequently, shallow-water theory is reformulated in terms of a distinguished limit which expresses the controlling influence of the combined action of film transport and internal friction. The effect of bottom friction is also fully retained. In the case of thin films, our treatment is shown to lead to a parabolic film equation, for which the problems of degeneracy and ill-posedness arise.

The effects of film transport and film viscosity are expressed in terms of a Péclet number *Pe* and the Schmidt number *Sc* which are defined as follows

$$Pe = v_0/v_s, \qquad Sc = \nu_0/D_0. \tag{46}$$

Here, v_0 designates a reference diffusion velocity of the film given in terms of the length h_0 and the diffusivity D_0 (*cf.* the scaling of the velocity as given by (9))

$$v_0 = D_0/h_0. \tag{47}$$

If D_0 is expressed in terms of v_0 and h_0, the inverse of *Sc* is found to be a Reynolds number $Re = 1/Sc = h_0 v_0/\nu_0$.

Due to the prevailing species gradient in the film, the velocity v_0 characterizes film transport by diffusion in the transverse direction. Transport in longitudinal directions is by film-flow processes due to gradients in the pressure $p_h = p + \Pi(h)$. In order to set up a simple model, the liquid of the film is assumed to be barotropic and incompressible, *i.e.* $p = p(\rho) = $ const. Consequently, longitudinal film flow corresponds to processes of spreading and retraction driven by gradients in the disjoining pressure $\Pi(h)$, which in fact correspond to wetting phenomena [3]. As will be shown subsequently (see (103)), longitudinal flow in thin films represents a generalized diffusion process given in terms of a diffusion coefficient $D^l \sim \partial p_h'/\partial h'$. Consequently, the characteristic velocity v_s of longitudinal flow is given by

$$v_s' = \sqrt{(h'/\rho)\partial p_h'/\partial h'}. \tag{48}$$

As before, primes indicate dimension variables.

Since v_0, v_s characterize transport processes which cross at right angles, *Pe* of Equation (46) corresponds to a Péclet number as defined in convective diffusion in liquid boundary layers [5]. The definition of v_s by Equation (48) is based on $p_h = p + \Pi$ representing a function of h exclusively. That this is in fact the case for thin films will be shown shortly. Further, $p_h = p_h(h)$ represents a constitutive relationship which resembles $p = p(\rho)$ for ordinary barotropic fluids, pointing to an analogy between h (for thin films) and ρ (for ordinary barotropic fluids) which was already noticed in shallow-water hydraulics [28]. Consequently, the velocity v_s closely resembles the sound speed in ordinary barotropic liquids which gives the speed of propagation of weak pressure fluctuations. In the present case, the pressure fluctuations arise due to changes in the layer thickness h.

Based on the definitions of *Pe* and *Sc*, the controlling influence of species diffusion and film viscosity are expressed by

$$Pe \ll 1, \quad Sc \gg 1, \quad \text{with } 1/Sc\,Pe^2 = O(1). \tag{49}$$

The condition of viscosity being high in comparison with film diffusivity $(Sc \gg 1)$ ensures that transverse transport is by diffusion. The condition of $Pe \ll 1$ ensures that transverse diffusion is slow in comparison with longitudinal film flow. Thin-film dynamics are treated in the limit $Pe \to 0$ and $Sc \to \infty$ which is a distinguished limit, since $1/(Sc\,Pe^2)$ is to remain an $O(1)$-quantity.

In order to investigate this distinguished limit, the Navier–Stokes equations for the flow field are rewritten in terms of Pe and Sc. For the case of $p_h = p_h(h)$, Equation (7) gives

$$(\partial_t + \vec{v} \cdot \nabla)\vec{v} = Sc\left(-\frac{\partial p_h}{\partial h}\nabla h + \nabla^2 \vec{v}\right). \tag{50}$$

Since v_s is defined by (48) in terms of dimensional variables, we find

$$\frac{1}{Sc\,Pe^2} = \frac{h_0}{\nu_0 v_0}\frac{h'}{\rho}\frac{\partial(p_h)'}{\partial h'} = h\frac{\partial p_h}{\partial h}. \tag{51}$$

Equation (50) is therefore found to become

$$(\partial_t + \vec{v} \cdot \nabla)\vec{v} = Sc\left(-\frac{1}{Sc\,Pe^2}\frac{1}{h}\nabla h + \nabla^2 \vec{v}\right). \tag{52}$$

In the distinguished limit as defined by (49), we therefore obtain

$$-\frac{\partial p_h}{\partial h}\nabla h + \nabla^2 \vec{v} = 0. \tag{53}$$

It is worth noting that shallow-water theory treats the opposite case of $Re \gg 1$ ([28]).

The distinguished limit defined by (49) leading to the reduced form of the Navier–Stokes equations as given by (53) may be derived in the form of a long-wave limit, *i.e.* with the help of the method of strained coordinates [29]. If l_0 is defined to represent a length characterizing the structures of the film, then for large structures, a small parameter a is given by

$$a = h_0/l_0 \ll 1. \tag{54}$$

In order to describe longitudinal flows along the surface of the substrate, a 'strained' representation of independent and dependent variables is introduced. For the coordinates x_1, x_2, z and the velocity $\vec{v} = \{u_1, u_2, w\}$ we choose

$$\left.\begin{array}{l} \{x_1, x_2, z\} \to \{a^{-1}x_1, a^{-1}x_2, z\} \\ \{u_1, u_2, w\} \to \{u_1, u_2, aw\} \end{array}\right\}. \tag{55}$$

The condition of high viscosity, *i.e.* $Sc \gg 1$, leads to transport processes being slow. These are therefore represented in terms of a slow diffusion time defined by

$$t \to (1/a)t. \tag{56}$$

Due to the transformation of (9) which resulted in the dimensionless time $(t = h_0^2 t'/D_0)$, the limit $t \to t/a$ is seen to be equivalent to

$$D_0 \to a D_0. \tag{57}$$

Consequently, the operator $(\partial_t + \vec{v} \cdot \nabla)$ which determines temporal change on the left-hand sides of (5–7) results in strained coordinates as follows

$$(\partial_t + \vec{v} \cdot \nabla) \to a(\partial_t + \vec{u} \cdot \nabla_s + w\partial_z). \tag{58}$$

In strained variables, Equation (7) is found to give

$$a(\partial_t + \vec{u} \cdot \nabla_s + w\partial_z)\{u_1, u_2, aw\}$$
$$= -\{a\partial_{x_1}, a\partial_{x_2}, \partial_z\}(p + \Pi) + (a^2\partial_{x_1}^2 + a^2\partial_{x_2}^2 + \partial_z^2)\{u_1, u_2, aw\}. \tag{59}$$

The requirement of $1/(Sc\,Pe^2) = O(1)$ necessitates that the pressure $p + \Pi$ is also to be strained, so that straining is applied to the independent and also to some of the dependent variables [29]

$$p + \Pi \to (1/a)(p + \Pi). \tag{60}$$

Under the condition of Equation (60), the following equations result from (59) in zeroth and first order with respect to a

$$\partial_z(p + \Pi) = 0, \tag{61}$$

$$-\nabla_s(p + \Pi) + \partial_z^2 \vec{u} = 0. \tag{62}$$

In (62), $\nabla_s = \{\partial_{x_1}, \partial_{x_2}, 0\}$ designates the surface nabla and $\vec{u} = \{u_1, u_2, 0\}$ the longitudinal velocity field.

Equation (61) shows that $p + \Pi = p_h$ represents a function of h exclusively. Therefore, a Péclet number based on the velocity as defined by (48) is a useful concept.

Since $(p + \Pi)$ is independent of z according to (61), integration of (62) is straightforward. The constants of integration may be found from (33) and (44).

For a surface given by $z = h(x_1, x_2, t)$ spanning the (x_1, x_2)-plane, the vectors $\vec{n}$ and $\vec{t}$ of normal and tangent (Figure 2) are found to be

$$\left. \begin{aligned} \vec{n} &= \{-a\partial_{x_1}h, -a\partial_{x_2}h, 1\}\frac{1}{\sqrt{1 + a^2(\nabla_s h)^2}} \\ \vec{t} &= \{-a\partial_{x_2}h, a\partial_{x_1}h, 0\}\frac{1}{a\sqrt{(\nabla_s h)^2}} \end{aligned} \right\}. \tag{63}$$

To lowest order in a, the deformation tensor $\mathbf{D} = (\nabla\vec{v})^+$ is found to be

$$\mathbf{D} = \frac{1}{2}\begin{pmatrix} 0 & 0 & u_{1,z} \\ 0 & 0 & u_{2,z} \\ u_{1,z} & u_{2,z} & 0 \end{pmatrix}. \tag{64}$$

Consequently,

$$\mathbf{D} \cdot \vec{n} = \partial_z \vec{u}, \qquad \vec{n} \cdot \mathbf{D} \cdot \vec{n} = 0. \tag{65}$$

Use of (65) transforms the stress boundary conditions (32) and (33) at the top surface, which gives

$$z = h: \begin{cases} (1/a)p = \sigma\kappa = \sigma\nabla_s \cdot \vec{n} = -\sigma a^2\nabla_s^2 h, \\ \partial_z\vec{u} = -\nabla_s\sigma = -(\partial\sigma/\partial T)a\nabla_s T. \end{cases} \tag{66}$$

In (66), the surface gradient is expressed with the help of ∇_s in the form of a directional derivative. Particularly, $\nabla_s\sigma = (\mathrm{d}\sigma/\mathrm{d}s)\vec{t}$ and $\nabla_s T = (\mathrm{d}T/\mathrm{d}s)\vec{t}$.

Surface tension is assumed to be primarily determined by the surface temperature, *i.e.* $\sigma = \sigma(T)$. Therefore, $\nabla_s\sigma$ may be expressed in terms of a Marangoni-number M defined as

$$M = (\partial\sigma/\partial T). \tag{67}$$

In order to retain the influence of surface tension and of the Marangoni effect in Equation (66), σ and M have to be strained along with $(p + \Pi)$ in the following manner

$$\sigma \to (1/a^3)\sigma, \qquad M \to (1/a)M. \tag{68}$$

In the strained variables, Equations (66) are found to give

$$z = h: \begin{cases} p = -\sigma\nabla_s^2 h, \\ \partial_z\vec{u} = -M\nabla_s T. \end{cases} \tag{69}$$

The conditions at the outer surface of the film for the solution $\vec{u}$ of (62) is thus found to be given in terms of the surface temperature $T|_{z=h} = T_h$ which is yet to be determined. By way of their boundary conditions, temperature T and species concentration C are coupled, which complicates their derivation. The field equations, on the other hand, are easily integrated, since they turn out to be linear due to $D_0 \to aD_0$ according to Equation (57).

Use of the strained variables of (55, 56) in (5) is found to give the following field equation for the species concentration C in lowest order in a

$$\partial_z^2 C = 0, \tag{70}$$

with the following boundary conditions according to (26) and (41)

$$C|_{z=h} = 1, \qquad C|_{z=0} = 0. \tag{71}$$

Consequently, the solution of (70) is found to be

$$C = z/h. \tag{72}$$

Equation (72) leads to a parabolic reaction law [2].

If the strained variables as defined in (55) and (56) are used in (6), then the lowest order in a of the temperature field T is found to be given by

$$\partial_z^2 T = 0. \tag{73}$$

For the temperature field T, the boundary condition at the top surface of the film is given by (39), which to lowest order in a reduces to

$$z = h: \psi(1 + \Lambda T) + \partial_z T + Bi(T - T_\infty) = 0. \tag{74}$$

For Equation (74), $J = \psi(1 + \Lambda T|_{z=h})$ according to (18) has been used.

The boundary condition for T at the bottom is provided by (45), which to lowest order in a gives

$$z = 0: \partial_z T - Bi_f(T - T_f) + Q_f\gamma I = 0. \tag{75}$$

According to (43) and (72), I is given by

$$z = 0: I = d\,\partial_z C = d/h. \tag{76}$$

The two constants of integration α, β for the general solution of Equation (73),

$$T = \alpha z + \beta, \tag{77}$$

are determined from the following two equations derived from (74–76)

$$\left.\begin{array}{l} z = h: \psi(1 + \Lambda\alpha h + \Lambda\beta) + \alpha + Bi(\alpha h + \beta) - BiT_\infty = 0 \\ z = 0: \alpha - Bi_f\beta + Bi_fT_f + Q_f\gamma d/h = 0 \end{array}\right\}. \tag{78}$$

For $z = h$, the surface temperature $T_h = T|_{z=h}$ of the film is given as $T_h = \alpha h + \beta$ because of (77). In terms of the solution for α, β of Equation (78) T_h is found to be

$$T_h = \frac{(-Bi_f\psi + Bi\,Bi_fT_\infty)h^2 + (Bi_fT_f + BiT_\infty - \psi)h + Q_f\gamma d}{hBi_f(\psi\Lambda + Bi)(h + 1/Bi_f + 1/(\psi\Lambda + Bi))}. \tag{79}$$

From (7), the Navier–Stokes equations result in strained variables (see (55) and (56)) in reduced form as given by (53) for the longitudinal flow field $\vec{u} = \{u_1, u_2, 0\}$. Our long-wave approximation is thus found to correspond to the distinguished limit as defined by (49). With the boundary conditions as given by (44) (for $z = 0$) and (69) (for $z = h$), we find

$$\left.\begin{array}{l} \partial_z^2\vec{u} = \nabla_s p_h, \qquad \vec{u}|_{z=0} = 0 \\ \partial_z u|_{z=h} = -M\nabla_s T = -M(\partial T/\partial h)\nabla_s h \end{array}\right\}. \tag{80}$$

From (80), the solution $\vec{u}(z; h)$ is found to be

$$\vec{u}(z; h) = \frac{z^2}{2}\nabla_s p_h + z\left(-M\frac{\partial T_h}{\partial h}\nabla_s h - h\nabla_s p_h\right). \tag{81}$$

According to (69), $p = -\sigma\nabla_s^2 h$. Therefore $p_h = p + \Pi = -\sigma\nabla_s^2 h + \Pi(h)$, so the surface gradient of p_h becomes

$$\nabla_s p_h = -\sigma\nabla_s^3 h + \frac{\partial\Pi}{\partial h}\nabla_s h. \tag{82}$$

Use of (82) in (81) gives the complete expression for $\vec{u}(z; h)$ as

$$\vec{u}(z; h) = -zM\frac{\partial T_h}{\partial h}\nabla_s h + (-hz + z^2/2)\left[-\sigma\nabla_s^3 h + \frac{\partial\Pi}{\partial h}\nabla_s h\right], \tag{83}$$

where $T_h = T_h(h)$ is given by (79).

For the determination of $\vec{u}$ to be complete, the unknown film thickness h is yet to be found. Since the functional dependence of $\vec{u}$ on z is known from (83), the continuity equation (4) may be integrated with respect to z to give the so-called 'film equation' which determines the spatio-temporal evolution of the thickness h. This approach is in close parallel to shallow-water theory, where the integration of the continuity equation with respect to the transverse coordinate also leads to a film equation [28]. The film equation will be derived in the next section.

5. The surface representation of film flow

The continuity equation (4) in strained variables (55) gives

$$\nabla_s \cdot \vec{u} + \partial_z w = 0. \tag{84}$$

Equation (84) may be integrated across the film with respect to the transverse coordinate z

$$w_h = w_0 - \int_0^h (\nabla_s \cdot \vec{u})\, \mathrm{d}z, \tag{85}$$

where w_0 and w_h designate the transverse components of the velocity field at $z = 0$ and $z = h$.

At $z = 0$, Equation (42) may be expressed in strained variables (55) which gives

$$-aw_0 = E(I + J) = E(1 - \gamma)I. \tag{86}$$

Also, in strained variables (43) is found to give

$$d\partial_z C|_{z=0} = I = d/h, \tag{87}$$

where (72) has been used. Consequently, in order to retain a contribution due to the chemical reaction on the surface of the substrate at $z = 0$, the parameter E needs to be strained also

$$E \to aE. \tag{88}$$

In terms of strained variables, w_0 is then obtained from (86–88) as follows

$$w_0 = -dE(1 - \gamma)/h. \tag{89}$$

At $z = h$, surface kinematics is expressed by (23). It may be combined with (24), to give

$$\partial_t h + (E(J + I) - \vec{n} \cdot \vec{v})\sqrt{1 + (\nabla_s h)^2} = 0. \tag{90}$$

In strained variables (55, 56, 63 and 68), Equation (90) is found to give

$$\partial_t h + [E(J + I) + \vec{u} \cdot \nabla_s h - w_h] = 0. \tag{91}$$

Use of (89) and (91) in Equation (85) gives

$$\partial_t h + [E(J + I) + \vec{u} \cdot \nabla_s h]_{z=h} + \frac{dE(1 - \gamma)}{h} + \int_0^h (\nabla_s \cdot \vec{u})\, \mathrm{d}z = 0. \tag{92}$$

Equation (92) may be transformed by means of the Leibniz formula in the following form

$$\nabla_s \cdot \int_0^h \vec{u} \, dz = \int_0^h (\nabla_s \cdot \vec{u}) \, dz + \vec{u} \cdot \nabla_s h|_{z=h}.$$

Equation (92) is then found to give

$$\partial_t + \nabla_s \cdot \int_0^h \vec{u} \, dz + E(J + I)_{z=h} + \frac{d \, E(1 - \gamma)}{h} = 0. \tag{93}$$

For (93), $J = \psi(1 + \Lambda T_h)$ according to Equation (18), with T_h given by (79).

In order to find I at $z = h$, Equation (25) has to be expressed in strained variables. Use of (55, 63, 71 and 72) and restriction to lowest order gives

$$I = -d \, \partial_z C|_{z=h} = -d/h. \tag{94}$$

Consequently, Equation (93) represents a closed evolution equation for h, determining the contribution which is of first order in a. If (94) is inserted in (93), we find

$$\partial_t h + \nabla_s \cdot \int_0^h \vec{u} \, dz + EJ - dE\gamma/h = 0. \tag{95}$$

Thus we find that integration of the continuity equation with respect to the transverse coordinate z (see (85)) results in a surface evolution equation as given by (95) which is of primary interest, since its solution $h(\vec{x}, t)$ leads to a complete determination of the thermo-hydrodynamics of the transport problem for the thin surface layer.

Particularly,

$$\vec{Q} = \int_0^h \vec{u} \, dz \tag{96}$$

represents a surface flux, while the sink term EJ accounts for the vaporization losses of the layer and the source term $dE\gamma/h$ gives the layer growth due to chemical reaction. Due to its inverse dependence on h, the source term corresponds to what is known as a parabolic reaction law in heterogeneous combustion.

An integration of the expression for $\vec{u}$ as given by (83) is found to give the surface flux $\vec{Q}$ according to (96)

$$\vec{Q} = - hM \frac{\partial T_h}{\partial h} \nabla_s h + \frac{h^3}{3} \left[\sigma \nabla_s^3 h - \frac{\partial \Pi}{\partial h} \nabla_s h \right]. \tag{97}$$

To lowest order in terms of a, the film equation is finally obtained in the form of a partial differential equation for h which is of the parabolic type

$$\partial_t h + \nabla_s \cdot \left[\left(- \frac{h^3}{3} \frac{\partial \Pi}{\partial h} + \frac{h^3}{3} \sigma (\nabla_s \nabla_s) - hM \frac{\partial T_h}{\partial h} \right) \cdot \nabla_s h \right] + EJ - dE\frac{\gamma}{h} = 0. \tag{98}$$

Equation (98) represents the surface flow of a liquid layer in the form of a generalized reaction-diffusion process for the thickness h, with diffusion coefficient D^l defined by

$$D^l = \frac{h^3}{3} \sigma (\nabla_s \nabla_s) - \frac{h^3}{3} \frac{\partial \Pi}{\partial h} - hM \frac{\partial T_h}{\partial h}. \tag{99}$$

In terms of D^l, Equation (98) becomes finally

$$\partial_t h + \nabla_s \cdot [D^l(h)\nabla_s h] + (1/\rho)(w_{\text{vap}} - w_{\text{form}}) = 0, \tag{100}$$

where w_{vap}, w_{form} represent the rate of film vaporization and the rate of film formation as introduced in Section 1. In the long-wave approximation, we therefore find

$$w_{\text{vap}} = \rho E J, \qquad w_{\text{form}} = \rho \gamma dE(1/h). \tag{101}$$

The diffusion coefficient D^l (see (99)) actually represents a differential operator, which corresponds to what is commonly found for nonuniform systems by employing 'gradient theory' [25, 30].

Our final equation (100) is given in terms of strained dimensionless variables. The independent variables $\vec{x}$, z, t and pressure p, mass fraction c of oxygen, temperature T were made dimensionless by Equations (9) and (11). The coordinates $\vec{x}$, z, t were then strained by (55) and (56), as were the pressures p, Π according to (60), the surface tension σ and the Marangoni number M according to (68), and the parameter E as defined by (24) according to (88). In order to avoid clutter, no new letters were introduced to distinguish the strained from the unstrained parameters.

If Marangoni effect and surface tension in the top surface of the layer are neglected (*i.e.* $M = 0$, $\sigma = 0$), then D^l is given as

$$D^l = -\frac{h^3}{3}\frac{\partial \Pi}{\partial h}. \tag{102}$$

According to Equation (61): $p_h = p(\rho) + \Pi(h)$. For incompressible liquids $\rho = \text{const.}$ and hence we find

$$D^l = -\frac{h^3}{3}\frac{\partial p_h}{\partial h}. \tag{103}$$

Due to (103), the introduction (as in (48)) of the reference velocity v_s characterizing surface flow is found to be justified, since $D^l \sim v_s^2$.

For the particular case of mesoscopic layers with $\Pi(h)$ given by (8), D^l is found to be

$$D^l = (\alpha/h). \tag{104}$$

Equation (100) represents a reaction-diffusion equation. Since both the sink and the source term are functions of h, special values h_i, $(i = 1, 2, \ldots)$ exist for which

$$J - d(\gamma/h) = 0. \tag{105}$$

Consequently, solutions of Equation (100) exist which are stationary films of constant thickness h. These solutions define 'dissipative phases', so that general evolutions of the layer may be interpreted in terms of coexistent dissipative surface phases for which phase transitions, *i.e.* surface waves in the layer thickness, occur. Such an approach permits to bring in the methods developed for the treatment of dynamical phase transitions [31] and for the description of pattern formation in reaction-diffusion systems [32]. For thin films on reaction surfaces, this approach has been investigated in [33, 34].

6. Conclusion

It has been shown that the long-wave approximation for thin films on reaction surfaces is the result of the application of a straining transformation which involves the independent variables (55, 56) and certain dependent variables and parameters of the problem (60, 68 and 88). This approach is shown to correspond to a distinguished limit defined in terms of a Péclet number and a Schmidt number, leading to a generalized reaction-diffusion equation for the evolution of the layer thickness h (100) from which a complete solution for the thermo-hydrodynamics of the layer is obtained. Since there may be an equilibrium, for certain values of the thickness h, between film generation due to chemical reaction and film removal due to evaporation, the introduction of the concept of dissipative phases in the form of stationary uniform layers is justified. It is useful, since the thermo-hydrodynamics of liquid layers covering reaction surfaces may then be treated by the application of advanced methods by which an understanding of the dynamics of transitions of ordinary phases was achieved.

References

1. G. H. Markstein, Heterogeneous reaction processes in metal combustion. In: *11th-Combustion Symposium 1967*. Philadelphia: The Combustion Institute (1967) pp. 219–234.
2. A. W. Adamson, *Physical Chemistry of Surfaces*. New York: Wiley (1990) 777pp.
3. P. G. de Gennes, Wetting: statics and dynamics. *Rev. Mod. Phys.* 57 (1985) 827–863.
4. J. P. Burelbach, S. G. Bankoff and S.H. Davis, Nonlinear stability of evaporating/condensing liquid films. *J. Fluid Mech.* 195 (1988) 463–499.
5. V. G. Levich, *Physicochemical Hydrodynamics*. Englewood Cliffs: Prentice-Hall (1962) 700pp.
6. D. A. Frank-Kamenetzkii, *Diffusion and Heat Transfer in Chemical Kinetics*. New York: Plenum (1969) 574pp.
7. J. Lighthill, *Waves in Fluids*. Cambridge: Cambridge University Press (1979) 504pp.
8. M. K. King, Ignition and combustion of boron particles and clouds. *J. Spacecraft Rockets* 19 (1982) 294–306.
9. C. K. Law, A simplified theoretical model for vapor phase combustion of metal particles. *Combust. Sci. Technol.* 7 (1973) 197–212.
10. A. Atkinson, Transport processes during the growth of oxide films at elevated temperatures. *Rev. Mod. Phys.* 57 (1985) 437–470.
11. M. K. King, A review of studies of boron ignition and combustion phenomena at Atlantic Research Corporation. In: K. K. Kuo and R. Pein (eds.), *Combustion of Boron-based Solid Propellants and Solid Fuels*. Boca Raton, CRC Press (1993) pp. 1–80.
12. P. W. Atkins, *Physical Chemistry*. Oxford: Oxford University Press (1983) 1095pp.
13. I. Glassman, F. A. Williams and P. Antaki, A physical and chemical interpretation of boron particle combustion. In: 19th-JANNAF Combustion Meeting, CPIA-Publ. No. 366, Vol. I (1982) 63–72.
14. A. Napolitano, P. B. Macedo, E. G. Hawkins, Viscosity and density of boron trioxide. *J. Amer. Ceram. Soc.* 48 (1965) 613–616.
15. G. K. Creffield and A. J. Wickens, Thermal conductivity of anhydrous borax, boric oxide and sodium sulfate. *J. Chem. Eng. Data* 20 (1975) 223–225.
16. M. K. King, Boron particle ignition in hot gas streams. *Combust. Sci. Technol.* 8 (1974) 255–273.
17. Gmelin System-No. 13 (Bor), 1st Suppl. Volume 1 (pp. 120–145). Weilheim: Verlag Chemie (1980) 503pp.
18. E. L. Dreizin and M. A. Trunov, Surface phenomena in aluminium combustion. *Combust. Flame* 101 (1995) 378–382.
19. M. A. Gurevich, I. M. Kiryanov and E. S. Ozerov, Combustion of individual boron particles. *Combust. Explos. Shock Waves* 5 (1969) 150–153.
20. M. Salita, Deficiencies and modelling of slag generation in solid rocket motors. *J. Propulsion Power* 11 (1995) 10–23.
21. K. Seshadri and D. E. Rosner, Polarization (ellipsometric) measurements of liquid condensate deposition and evaporation rates. *Combust. Flame* 61 (1985) 251–260.
22. J. I. Frenkel, *Kinetic Theory of Liquids*. New York: Dover (1955) 510pp.
23. M. D. Scheer, The molecular weight and vapor pressure of gaseous boron suboxide. *J. Phys. Chem.* 62 (1957) 490–493.

24. E. E. Shpilrain, K. A. Yakimov and A.F. Tsitsarkin, Surface tension of liquid boric oxide at up to 2100C. *High Temperature (USSR)* 12 (1974) 77–82.
25. J. S. Rowlinson and B. Widom, *Molecular Theory of Capillarity*. Oxford: Clarendon Press (1982) 327pp.
26. J. M. Delhaye, Jump conditions and entropy sources in two-phase systems. *Int. J. Multiphase Flow* 1 (1974) 395–409.
27. J. Bebernes and D. Eberly, *Mathematical Problems from Combustion*. New York: Springer-Verlag (1989) 177pp.
28. G. B. Whitham, *Linear and Nonlinear Waves*. New York: Wiley (1974) 636pp.
29. A. H. Nayfeh, *Perturbation Methods*. New York: Wiley (1973) 425pp.
30. S. H. Davis and L. E. Scriven, Stress and structure in fluid interfaces. *Adv. Chem. Phys.* 49 (1982) 357–454.
31. J. D. Gunton, M. San Miguel and P. S. Sahni, The dynamics of first order phase transitions. In: C. Domb and J.C. Lebowitz (eds.), *Phase Transitions and Critical Phenomena Vol. 8*. London: Academic Press (1983) pp. 269–466.
32. A. S. Mikhailov, *Foundations of Synergetics I*. Berlin: Springer-Verlag (1990) 187pp.
33. D. Meinköhn, The dynamics of thin films on reaction surfaces. *Combust. Sci. Technol.* 105 (1995) 85–116.
34. D. Meinköhn and A. S. Mikhailov, Pattern formation by surface chemical reactions. *Phys. Lett. A* 178 (1993) 143–149.